Biointerface Research in Applied Chemistry
Open-Access Journal (ISSN: 2069-5837)

Article
Volume 16, Issue 2, 2026, 41
https://doi.org/10.33263/BRIAC162.041

The Effect of *Sapindus rarak* Extract on the Structural and Morphological Properties of Zn_2SnO_4

Eka Angasa [1,*], Sal Prima Yudha [1], Charles Banon [1], Evi Maryanti [1], Rido Kurnia [2], Vivi Sisca [3]

[1] Department of Chemistry, Universitas Bengkulu, Bengkulu, Indonesia; eka.angasa@gmail.com (E.A.); sp.yudha.S@gmail.com (S.P.Y.); banonc89@yahoo.com (C.B.); evimaryanti82@yahoo.com (V.M.);
[2] Department of Pharmacy, Universitas Bengkulu, Bengkulu, Indonesia; ridhokurnia172018@gmail.com (R.K.);
[3] Research Center for Chemistry, National Research and Innovation Agency, Banten, Indonesia; vivii311084@gmail.com (V.S.);
* Correspondence: eka.angasa@gmail.com;

Received: 21.03.2025; Accepted: 22.04.2025; Published: 17.02.2026

Abstract: This study examined the effect of *Sapindus rarak* seed extract on the structure and morphology of Zn_2SnO_4 synthesized using the hydrothermal method. *Sapindus rarak* extract, containing saponins, flavonoids, and phenolic compounds, was employed as an environmentally friendly natural capping agent to replace synthetic surfactants. Based on the XRD pattern, the extract with a concentration of 2% produced Zn_2SnO_4 with high crystallinity, as evidenced by sharp and intense diffraction peaks. The ZnO phase appeared at an extract concentration of 4%, indicating a compositional change. SEM and TEM analyses revealed that *Sapindus rarak* extract had an effect on the morphology of Zn_2SnO_4 particles, resulting in spherical particles with a larger average size compared to samples synthesized without the extract. Active biomolecules in the extract contribute to regulating particle size, inhibiting agglomeration, and increasing material crystallinity. This study shows that *Sapindus rarak* extract has considerable potential as a natural resource for the environmentally friendly synthesis of nanomaterials. This sustainable and efficient method is optimal for a wide range of clean energy and environmental processing applications.

Keywords: Zn_2SnO_4; hydrothermal method; aqueous extract; *Sapindus rarak*.

1. Introduction

Because of its special qualities, including a wide band gap (3.6 eV), elevated electron mobility (10-15 $cm^2V^{-1}s^{-1}$), high electrical conductivity (~10^4 Scm^{-1}), attractive optical characteristics, and low light absorption, zinc tin oxide, represented by the chemical formula Zn_2SnO_4, has attracted much attention [1,2]. An efficient approach to control these properties during the synthesis process is the use of additives, such as surfactants and capping agents [4-6]. In previous studies [4,5], the surfactants included hexadecyltrimethylammonium bromide (CTAB) and L-tryptophan. Given the increasing environmental issues, advances in environmentally friendly nanoparticle synthesis techniques are crucial. Plant extracts have become a desirable alternative because they can limit, stabilize, and reduce the synthesis of nanomaterials [7,8]. Among these extracts, several active biochemical compounds are flavonoids, terpenoids, ketones, aldehydes, amides, and carboxylic acids. They have great

antioxidant activity for this reason as well. Plant extracts are easy to use, economical, and non-toxic, which are some of the benefits of plant extracts in material synthesis. These molecules can produce chelate interactions by transforming metal oxide ions into particles of different diameters and forms [9,10]. Particularly for the synthesis of additional metal oxide compounds, the use of plant extracts to generate materials with favorable properties should be investigated due to the advantages and environmentally friendly character of this method [11,12].

This study reported the use of *Sapindus rarak* seed extract in the synthesis of Zn_2SnO_4, in line with the aim of obtaining an environmentally friendly synthesis method. Because of its high saponin concentration, *Sapindus rarak*—also known as soapberry—has long been used naturally as a detergent in small-scale businesses in Indonesia [13]. Reducing surface tension [14,15] and acting as nanomaterial stabilizers and coatings [13,16], the seeds contain saponins and phenol derivatives [13]. This extract helps scientists synthesize spherical Zn_2SnO_4 particles.

2. Materials and Methods

2.1. Materials.

Zn_2SnO_4 was synthesized using analytical-grade reagents without additional purification. Zinc acetate dihydrate ($Zn(CH_3COO)_2.2H_2O$, purity ≥99.5%) and sodium hydroxide (NaOH) were obtained from Merck. Tin (IV) chloride ($SnCl_4$, purity 98%) was obtained from Sigma Aldrich. Rinds of *Sapindus rarak* were obtained from an online market in Situbondo, East Java, Indonesia.

2.2. Preparation of Extract.

Sapindus rarak seeds were thoroughly washed with tap water and subsequently rinsed with demineralized water. After washing, the seeds were naturally dried for one week and then blended using an electric blender. The blended seeds were weighed accordingly (1%, 2%, 3%, and 4% (w/v)), and demineralized water was added to reach a total volume of 100 mL. The mixture was heated at 70℃ for 1 hour under continuous stirring. After filtration, a clean brown solution of *Sapindus rarak* extract was obtained and stored in a refrigerator for further use in Zn_2SnO_4 synthesis.

2.3. Synthesis of Zn_2SnO_4.

As previously reported, zinc stannate powder was prepared using a hydrothermal process with minor modifications [17,18]. All chemical reagents were of analytical purity and were used without further purification. Typically, 10 mL of 0.2 M zinc acetate dihydrate was added to 10 mL of 0.1 M tin chloride under stirring (800 rpm) at room temperature for 10 minutes, resulting in the formation of a white suspension. Subsequently, 5 mL of aqueous extract was added to the mixture under continuous stirring for 10 minutes, followed by the addition of 20 mL of 0.4 M sodium hydroxide, maintaining a molar ratio of Zn: Sn: OH at 2:1:8. After 30 minutes of reaction, the final mixture was transferred into a Teflon-lined autoclave (100 mL capacity) and maintained at 185℃ for 16 hours. The autoclave was then allowed to cool to ambient temperature. The resulting precipitate was collected and thoroughly rinsed with demineralized water. Finally, the product was subsequently dried in an air oven at

85℃ for 15 hours and characterized using XRD, SEM, and TEM. A schematic representation of the synthesis procedure is shown in Figure 1.

Figure 1. Schematic representation of the Zn_2SnO_4 synthesis procedure using *Sapindus rarak* extract.

2.4. Characterization.

The XRD patterns of the synthesized Zn_2SnO_4 were recorded using an X-ray diffractometer (PANanalytical X'pert PRO) with Cu Kα radiation (λ = 1.5406 Å) in the diffraction angle range of 10-100°. The morphology of the synthesized Zn_2SnO_4 was examined using scanning electron microscopy (FEI Inspect-S50) and transmission electron microscopy (JEM-1400). The optical absorption spectrum of the Zn_2SnO_4 was analyzed using a UV-Vis diffuse reflectance spectrophotometer (Thermo Scientific Nicolet iS10).

3. Results and Discussion

The XRD patterns of synthesized Zn_2SnO_4 with and without various concentrations of *Sapindus rarak* seed extract are shown in Figure 2a. It was observed that the extract concentration significantly affected the crystallinity and phase composition of the samples. The higher-intensity, sharper, and narrower peaks of Zn_2SnO_4 obtained with the extract indicated better crystallinity than those of Zn_2SnO_4 synthesized without the extract. The highest crystallinity was achieved using 2% extract, after which it decreased with increasing extract concentration. The optimal extract concentration facilitated the formation of Zn_2SnO_4 nanoparticles and maintained their growth stability. However, at higher extract concentrations, interactions between organic compounds in the extract and precursor components disrupted the crystallization process [19]. This condition led to the formation of smaller, less regular crystals, thereby reducing the crystallinity of Zn_2SnO_4. At a concentration of 4%, the Zn_2SnO_4 peaks gradually disappeared, replaced by ZnO peaks, suggesting that organic compounds acted as reductants or metal ion binders. The type and concentration of components in the extract are one of the main factors determining the formation rate, size, and shape of the obtained Zn_2SnO_4 [20]. Bioactive compounds in an appropriate concentration form a complex structure with Zn^+ and Sn^+ ions, resulting in Zn_2SnO_4 as an intermediate compound before decomposing and recrystallizing to form Zn_2SnO_4. However, excessively high concentrations may interfere with the formation of the $ZnSn(OH)_6$ complex, preventing the formation of Zn_2SnO_4 [18,21,22]. This transition altered the X-ray diffraction pattern, leading to the dominance of the ZnO phase and a reduced presence of Zn_2SnO_4 in the material [23]. Up to a 3% extract concentration, no peaks corresponding to other compounds were observed, indicating that the obtained Zn_2SnO_4 was of high purity. All peaks from the synthesized Zn_2SnO_4, both with and without the extract,

were indexed perfectly to a face-centered cubic spinel Zn_2SnO_4 structure with the space group *Fd-3mS*. These peaks corresponded to JCPDS data number 01-073-1725. The Le Bail refinement study further confirmed the samples' purity, providing a more detailed profile of Zn_2SnO_4 and its crystallinity (Figure 2b). As shown in Figure 2b, the computed (red line) and observed (black circles) XRD patterns exhibited a high degree of agreement, as evidenced by the low-reliability factor values and minimal differences in the difference plot (green line) (R_p=5.84, R_{wp}=7.37, χ^2=0.84). To examine the effect of the extract on crystallinity, the crystallinity degree and crystallite size of the synthesized Zn_2SnO_4 using the Scherrer formula were determined, as listed in Table 1. The results indicated that the extract significantly affected the crystallinity and phase composition of Zn_2SnO_4.

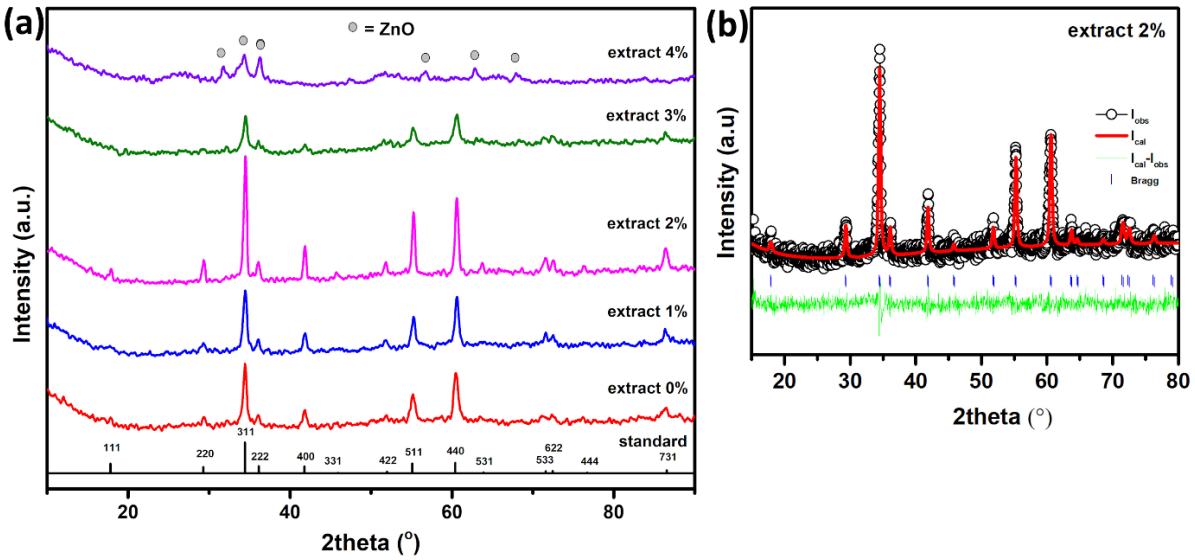

Figure 2. XRD pattern of Zn_2SnO_4 using *Sapindus rarak* extract: **(a)** XRD patterns with varying extract concentrations; **(b)** XRD Le Bail refinement for the sample prepared with 2% extract.

Table 1. Crystallinity degree and crystallite size of samples prepared with various quantities of Sapindus rarak extract.

Quantity of extract (%)	Phase	Degree of crystallinity (%)	Crystallite size (nm)
0	Zn_2SnO_4	23.61	9.09
1	Zn_2SnO_4	24.76	9.66
2	Zn_2SnO_4	29.84	11.27
3	Zn_2SnO_4	20.75	8.65
4	ZnO	18.18	7.63

Furthermore, the Le Bail refinement method was applied to the XRD data with varying quantities of extract to confirm its effect on the structure of the obtained Zn_2SnO_4, as shown in Table 2. Based on the refined data, the extract variation affected the lattice parameter values of all the obtained Zn_2SnO_4 samples. However, the Zn_2SnO_4 structure remained unchanged, as indicated by the consistent parameter values corresponding to the *Fd-3mS* space group and cubic crystal system. Changes in lattice parameter values reinforced the extract′s role in the nucleation, growth, and stabilization of Zn_2SnO_4, resulting in distinct a, b, and c values for each extract variation [17,19,24].

Table 2. Lattice parameters of Zn_2SnO_4 prepared using different extract concentrations and analyzed via the Le Bail refinement method.

Quantity of extract (%)	Space group	Crystal system	Z	Lattice parameter			
				a (Å)	b (Å)	c (Å)	V (Å^3)
0	Fd-3mS	Cubic	8	8.678	8.678	8.678	653.6
1	Fd-3mS	Cubic	8	8.673	8.673	8.673	652.5
2	Fd-3mS	Cubic	8	8.675	8.675	8.675	652.9
3	Fd-3mS	Cubic	8	8.680	8.680	8.680	653.9

Although the exact mechanism by which the extract affected metal oxide nanoparticle synthesis has not been fully understood, existing literature suggests that the biochemicals present in the *Sapindus rarak* extract, particularly saponin as the main component, play a crucial role in Zn_2SnO_4 nanoparticle formation [25,26]. Saponins and other compounds, such as alkaloids and terpenoids, contain active polar functional groups like carboxyl (-COOH), carbonyl (-C=O), amino (-NH_2), and hydroxyl (-OH) [21]. These bioactive compounds work synergistically to bind metal oxide ions through oxygen and other active sites, facilitating well-defined interactions. This process helps prevent particle agglomeration and promotes higher crystallinity in the synthesized Zn_2SnO_4 [22,27]. The presence of saponins in the extract was confirmed through FTIR analysis, as evidenced by the absorption peak at 1636 cm^{-1}, corresponding to the C=C stretching vibration originating from the aglycone in saponins (see Figure 3) [13,28]. Additionally, a broad peak at 3294 cm^{-1} indicated the stretching vibration of OH groups. The similar absorption peaks observed across all extract variations confirmed the presence of the same bioactive compounds.

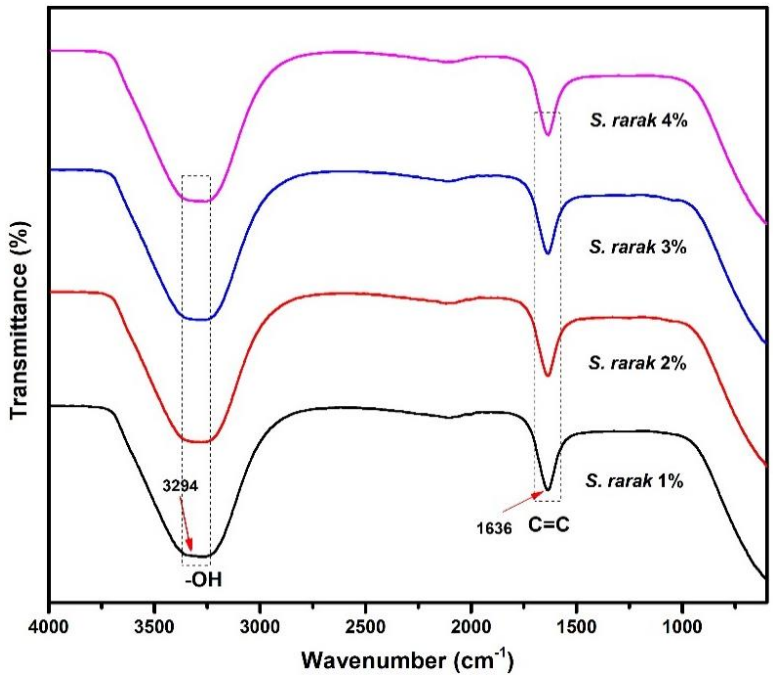

Figure 3. FTIR analysis of *Sapindus rarak* extract with varying quantities.

The morphology and size of the as-prepared Zn_2SnO_4 were investigated using SEM and TEM (Figure 4). The SEM images show that the Zn_2SnO_4 particles synthesized without the extract were agglomerated into irregular shapes (Figure 4a,b). However, TEM analysis confirmed that these particles exhibited an octahedron-like structure with an edge length range of 93-198 nm, with an average of 138 ± 38 nm as measured using ImageJ 1.52a software (Figure 4e). In contrast, the use of 2% extract led to a different outcome: particles were aggregated yet well dispersed, as shown in Figure 4c,d. TEM analysis further revealed that

Zn_2SnO_4 particles transformed into a spherical shape with a diameter range of 49-305 nm, with an average of 205 ± 86 nm (Figure 4f).

Aggregation of unmodified Zn_2SnO_4 nanoparticles could reduce their effectiveness in sensor and catalysis applications. However, the spherical shape of the Sapindus rarak extract prevented agglomeration and increased the material's active surface area and conductivity. This structural modification could improve the effectiveness of interactions and enhance the performance of materials in applications that rely on surface properties and reactivity [29]. Because different materials have different physicochemical properties, different particle sizes can adversely affect their performance and reproducibility. Scalability, environmental interaction, stability, and efficiency are all affected by this variability. Tight control of the synthesis process is necessary. Thus, techniques such as particle fractionation or coating materials should be applied to reduce particle size distribution and ensure more stable, better-performing performance [30].

These findings highlight the significance of the extract for altering the form of Zn_2SnO_4. During the synthesis of metal and metal oxide nanoparticles, the biomolecules in the extract are supposed to be a cover and a reducer. These biomolecules bind and immobilize metal ions during synthesis to generate nanoparticles of different sizes and shapes [27,31]. On the other hand, it is believed that the primary trigger of this morphological change in *Sapindus rarak* is rarasaponin, the main chemical present there. An important element in the formation of spherical Zn_2SnO_4 in *Sapindus rarak* extract is the stabilizing and reducing agent rarasaponin. The stabilizing effect of the saponin ensures a consistent particle size distribution and helps prevent particle clumping, thereby enhancing material reactivity and active surface area [25]. As reducing agents, saponins transform metal ions into oxide compounds, helping to produce controlled Zn_2SnO_4 nanoparticle crystals. The synergy between these two mechanisms leads to the development of Zn_2SnO_2 materials that exhibit superior quality and improved performance in various applications, such as energy storage, sensors, and photocatalysis [32].

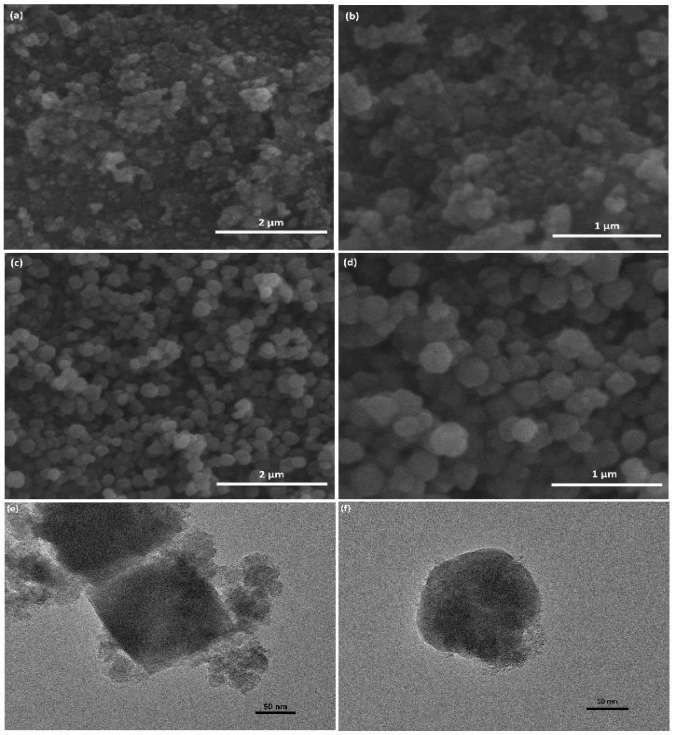

Figure 4. (a,b) SEM images of Zn_2SnO_4 prepared without extract; **(c,d)** SEM images of Zn_2SnO_4 prepared using 2% extract; **(e)** TEM images of Zn_2SnO_4 prepared without extract; **(f)** TEM images of Zn_2SnO_4 prepared using 2% extract.

Furthermore, the researchers investigated the effect of varying extract concentrations on Zn_2SnO_4 morphology, as illustrated in Figure 5. No significant changes in grain size and particle shape were observed when using extracts at concentrations of 1%, 3%, and 4%. These results indicated that a 2% extract concentration was optimal for producing Zn_2SnO_4 with well-defined grain boundaries. Table 3 summarizes the effects of different extract concentrations on the size and morphology of the synthesized Zn_2SnO_4 and compares them with commercial surfactants. Clearly, the *Sapindus rarak* extract has a significant impact on the formation of Zn_2SnO_4, which could further have great potential to replace the role of traditional surfactants as an eco-friendly and sustainable material. Different results were shown by previous research using extracts of *Impatiens balsamina* L. leaves and *Garcinia mangostana* fruit peels, which produced Zn_2SnO_4 in octahedral form with edge lengths of 160–350 nm and 600–900 nm, respectively [17,18]. This finding confirms that varying the extract components produces materials with specific shapes and sizes.

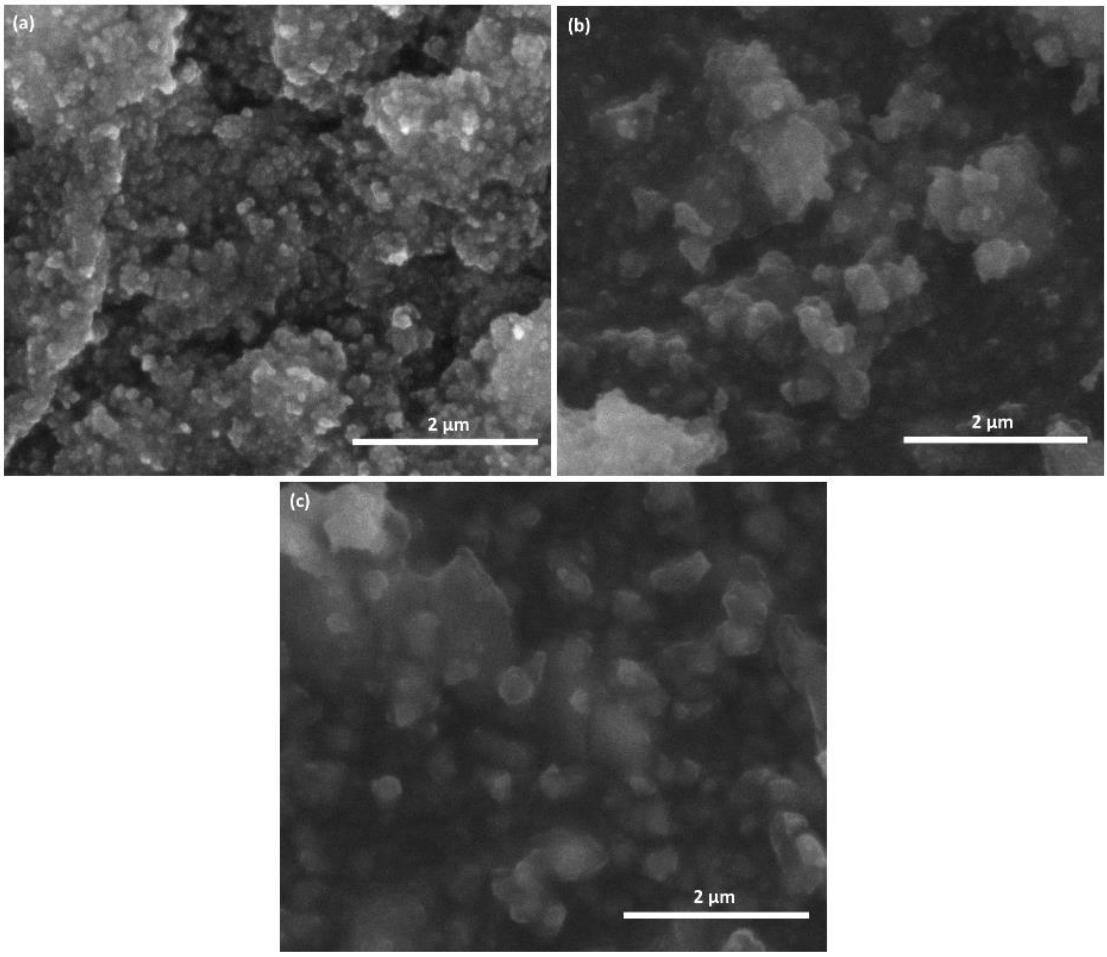

Figure 5. SEM images of as-prepared Zn_2SnO_4 with various extract concentrations: **(a)** 1%; **(b)** 3%; **(c)** 4%.

Table 3. Summary of as-prepared Zn_2SnO_4 characteristics with various extract concentrations and its comparison with commercial surfactants.

Type of surfactant		Morphology	Particle size (nm)	Ref
Sapindus rarak	0%	Agglomerated, octahedron-like	138 ± 38	**This research**
	1%	Agglomerated, irregular	-	
	2%	Well-defined grain size, spherical	205 ± 86	
	3%	Agglomerated, irregular	-	
CTAB		Well-defined grain size, cubic	133-332	[4]
L-tryptophan		Well-defined grain size, octahedral	~300	[33]
L-tryptophan		Well-defined grain size, cubic	100-150	[5]

After conducting XRD, SEM, and TEM analyses on all samples, the sample prepared with 2% extract demonstrated the most favorable characteristics. Consequently, this sample was chosen for further exploration of its optical properties. The optical properties of Zn_2SnO_4 prepared with and without 2% extract were evaluated using a UV-Vis DRS spectrophotometer (Figure 6). The band gap value was determined by the following equation:

$$E_g = \frac{hc}{\lambda} = \frac{1240}{\lambda} eV \quad (1)$$

Notes: Eg stands for the band gap energy (eV), λ for wavelength (nm), c for light speed (3×10^8 ms^{-1}), and h for Planck's constant (6.626×10^{-34} Js). Calculations revealed that Zn_2SnO_4 made with 2% extract had a band gap value (3.26 eV) lower than that of samples without extract (3.41 eV). The electronic structure of this sample changed with increasing crystallinity and particle size, and was closely associated with a decrease in the band gap [34]. Better light absorption in this sample suggests that photocatalytic uses would benefit from it.

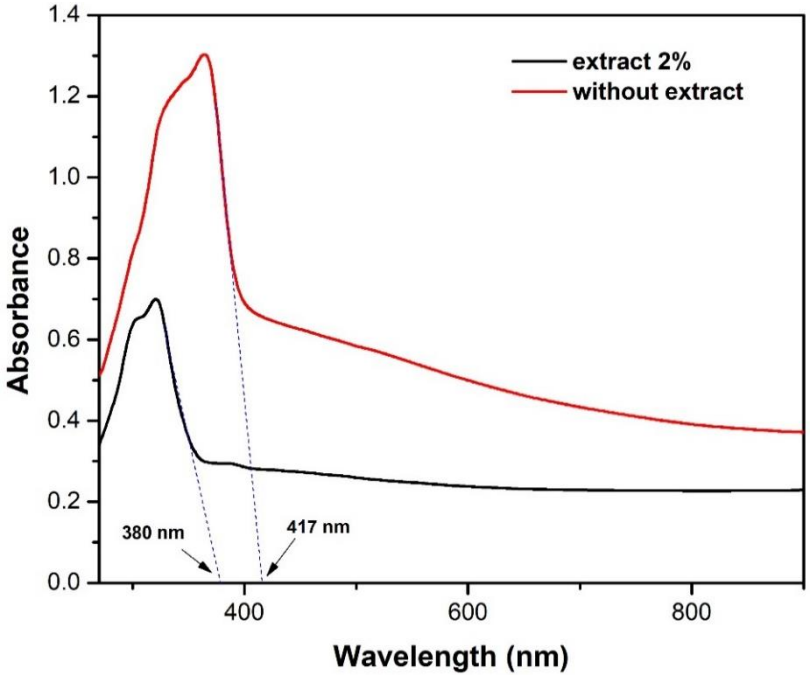

Figure 6. UV-Vis DRS spectra of Zn_2SnO_4 prepared with and without 2% extract.

The remarkable spherical character of Zn_2SnO_4 makes it appropriate for use in fields covering energy storage, sensors, and photocatalysis. The spherical form increases sensitivity, performance, interaction with target molecules, and active surface area of the material. Higher crystallinity improves ideal conductivity, which is critical for applications including energy storage and photocatalytic development. The spherical form of Zn_2SnO_4 lowers clumping, improving performance and stability in surface-oriented and reactivity applications. This raises the material's stability and efficiency progressively [35].

There is a major challenge to be solved when using plant extracts to make large-scale materials. Some of the most significant problems are the lack of access to raw materials, processing inefficiencies, variations in extract composition, and the challenge of scaling up the technology to meet industrial needs [36]. Solutions to these problems include establishing alternative sources of raw materials, optimizing synthesis processes, and using environmentally friendly technologies [37]. In addition, the scalability and reproducibility of green synthesis methods are hampered by variables in raw materials and uncertainties in process conditions, which can affect the consistency of results. Quality control and the complexity of technology

transfer hinder industrial-scale implementation. In addition, rising production costs due to large-scale operations continue to hamper method optimization [38].

4. Conclusions

The effective green synthesis of Zn_2SnO_4 was demonstrated in this study using the bark of *Sapindus rarak* as a covering material. XRD analysis showed that the *Sapindus rarak* extract retained its cubic structure and increased the crystallinity of Zn_2SnO_4. After adding 2% of the extract, SEM and TEM analysis showed that the agglomerated octahedral Zn_2SnO_4 nanoparticles formed without the extract were successfully converted into well-defined spherical particles with distinct grain boundaries. The Zn_2SnO_4 particles made without the extract and with the extract had sizes of 138 ± 38 nm and 205 ± 86 nm. These findings demonstrated that *the Sapindus rarak seed extract significantly improved* the structural and morphological characteristics of Zn_2SnO_4, making it more suitable for various applications.

Author Contributions

Conceptualization, E.A.; methodology, E.A. and S.P.Y.; software, E.A. and R.K.; validation, E.A., S.P.Y., and E.M.; formal analysis, E.A. and V.S.; investigation, E.A. and R.K.; resources, V.S.; data curation, E.A.; writing—original draft preparation, E.A.; writing—review and editing, E.A. and E.M.; visualization, C.B.; project administration, C.B.; supervision, E.A. All authors have read and agreed to the published version of the manuscript.

Institutional Review Board Statement

Not applicable.

Informed Consent Statement

Not applicable.

Data Availability Statement

Data supporting the findings of this study are available upon reasonable request from the corresponding author.

Funding

This research was funded by Universitas Bengkulu through the flagship research scheme under grant number 1976/UN30.15/PP/2022.

Acknowledgments

The authors thank the chemistry laboratory of Bengkulu University for its facility support during this research.

Conflicts of Interest

The authors declare that they have no known competing financial interests or personal relationships that could have appeared to influence the work reported in this paper.

References

1. Shi, L.; Dai, Y. Synthesis and photocatalytic activity of Zn_2SnO_4 nanotube arrays. *J. Mater. Chem. A* **2013**, *1*, 12981-12986, https://doi.org/10.1039/c3ta12388j.
2. Hwang, D.; Jin, J.-S.; Lee, H.; Kim, H.-J.; Chung, H.; Kim, D.Y.; Jang, S.-Y.; Kim, D. Hierarchically Structured Zn_2SnO_4 Nanobeads for High-Efficiency Dye-Sensitized Solar Cells. *Sci. Rep.* **2014**, *4*, 7353, https://doi.org/10.1038/srep07353.
3. Cinar, I. Improving structural and magnetic properties of zinc stannate thin films through nickel doping via sol–gel method. *Sci. Rep.* **2024**, *14*, 14808, https://doi.org/10.1038/s41598-024-63209-2.
4. Yuan, Z.; Yang, C.; Li, Y.; Meng, F.; Duan, J. Ppb-Level 2-Butanone Gas Sensor Based on CTAB-Assisted Synthesis of Small-Size ZnSnO Nano Cube. *IEEE Sens. J.* **2022**, *22*, 20156-20164, https://doi.org/10.1109/JSEN.2022.3199397.
5. Wang, Y.; Xu, F.; Sun, L.; Li, Y.; Liao, L.; Guan, Y.; Lao, J.; Yang, Y.; Zhou, T.; Wang, Y.; Li, B.; Zhang, K.; Zou, Y. A highly active Z-scheme SnS/Zn_2SnO_4 photocatalyst fabricated for methylene blue degradation. *RSC Adv.* **2022**, *12*, 31985-31995, https://doi.org/10.1039/d2ra05519h.
6. Sun, S.; Liang, S. Morphological zinc stannate: synthesis, fundamental properties and applications. *J. Mater. Chem. A* **2017**, *5*, 20534-20560, https://doi.org/10.1039/C7TA06221D.
7. Abada, E.; Mashraqi, A.; Modafer, Y.; Al Abboud, M.A.; El-Shabasy, A. Review green synthesis of silver nanoparticles by using plant extracts and their antimicrobial activity. *Saudi J. Biol. Sci.* **2024**, *31*, 103877, https://doi.org/10.1016/j.sjbs.2023.103877.
8. Haldar, A.G.M.; Mahapatra, D.K.; Dadure, K.M.; Chaudhary, R.G. Natural Extracts-mediated Biosynthesis of Zinc Oxide Nanoparticles and Their Multiple Pharmacotherapeutic Perspectives. *Jordan J. Phys.* **2022**, *15*, 67–79, https://doi.org/10.47011/15.1.10.
9. D'Souza, J.N.; Nagaraja, G.K.; Prabhu, A.; Navada, K.M.; Kouser, S.; Manasa, D.J. *Sauropus androgynus* (L.) leaf phytochemical activated biocompatible zinc oxide nanoparticles: An antineoplastic agent against human triple negative breast cancer and a potent nanocatalyst for dye degradation. *Appl. Surf. Sci.* **2021**, *552*, 149429, https://doi.org/10.1016/j.apsusc.2021.149429.
10. Radulescu, D.-M.; Surdu, V.-A.; Ficai, A.; Ficai, D.; Grumezescu, A.-M.; Andronescu, E. Green Synthesis of Metal and Metal Oxide Nanoparticles: A Review of the Principles and Biomedical Applications. *Int. J. Mol. Sci.* **2023**, *24*, 15397, https://doi.org/10.3390/ijms242015397.
11. Elkhateeb, O.; Atta, M.B.; Mahmoud, E. Biosynthesis of iron oxide nanoparticles using plant extracts and evaluation of their antibacterial activity. *AMB Expr.* **2024**, *14*, 92, https://doi.org/10.1186/s13568-024-01746-9.
12. Yadeta Gemachu, L.; Lealem Birhanu, A. Green synthesis of ZnO, CuO and NiO nanoparticles using *Neem leaf extract* and comparing their photocatalytic activity under solar irradiation. *Green Chem. Lett. Rev.* **2024**, *17*, 2293841, https://doi.org/10.1080/17518253.2023.2293841.
13. Aziz, A.; Andini Putri, B.G.; Prasetyoko, D.; Nugraha, R.E.; Holilah, H.; Bahruji, H.; Jalil, A.A.; Suprapto, S.; Hartati, H.; Asikin-Mijan, N. Synthesis of mesoporous zeolite Y using *Sapindus rarak* extract as natural organic surfactant for deoxygenation of *Reutealis trisperma* oil to biofuel. *RSC Adv.* **2023**, *13*, 32648-32659, https://doi.org/10.1039/d3ra05390c.
14. Wisetkomolmat, J.; Suksathan, R.; Puangpradab, R.; Kunasakdakul, K.; Jantanasakulwong, K.; Rachtanapun, P.; Sommano, S.R. Natural Surfactant Saponin from Tissue of *Litsea glutinosa* and Its Alternative Sustainable Production. *Plants* **2020**, *9*, 1521, https://doi.org/10.3390/plants9111521.
15. Wisetkomolmat, J.; Suppakittpaisarn, P.; Sommano, S.R. Detergent Plants of Northern Thailand: Potential Sources of Natural Saponins. *Resources* **2019**, *8*, 10, https://doi.org/10.3390/resources8010010.
16. Putro, J.N.; Ismadji, S.; Gunarto, C.; Soetaredjo, F.E.; Ju, Y.H. Effect of natural and synthetic surfactants on polysaccharide nanoparticles: Hydrophobic drug loading, release, and cytotoxic studies. *Colloids Surf. A: Physicochem. Eng. Asp.* **2019**, *578*, 123618, https://doi.org/10.1016/j.colsurfa.2019.123618.
17. Angasa, E.; Asdim; Zulhadjri; Jamarun, N.; Arief, S. The effect of *Impatiens balsamina* L. extract on structural, morphological, optical, and photocatalytic properties of Zn_2SnO_4. *J. Mater. Res. Technol.* **2020**, *9*, 12917–12925, https://doi.org/10.1016/j.jmrt.2020.09.017.
18. Angasa, E.; Putri, Y.E.; Zulhadjri; Jamarun, N.; Arief, S. Improving the morphological, optical, and photocatalytic properties of octahedral Zn_2SnO_4 using *Garcinia mangostana* fruit peel extract. *Vacuum* **2020**, *182*, 109719, https://doi.org/10.1016/j.vacuum.2020.109719.
19. Dey, S.; Mohanty, D.l.; Divya, N.; Bakshi, V.; Mohanty, A.; Rath, D.; Das, S.; Mondal, A.; Roy, S.; Sabui,

R. A critical review on zinc oxide nanoparticles: Synthesis, properties and biomedical applications. *Intell. Pharm.* **2025**, *3*, 53-70, https://doi.org/10.1016/j.ipha.2024.08.004.
20. Sadia, S.I.; Shishir, M.K.H.; Ahmed, S.; Alam, M.A.; Al-Reza, S.M.; Afrin, S.; Pappu, A.A.; Jahan, S.A. Green synthesis of crystalline silver nanoparticle by bio-mediated plant extract: A critical perspective analysis. *Nano-Struct. Nano-Objects* **2024**, *39*, 101272, https://doi.org/10.1016/j.nanoso.2024.101272.
21. Umar, A.; Sabrina, V.; Yulizar, Y. Synthesis of ZnO nanoparticles using *Sapindus rarak* DC fruit pericarp extract for rhodamine B photodegradation. *Inorg. Chem. Commun.* **2022**, *141*, 109593, https://doi.org/10.1016/j.inoche.2022.109593.
22. Ashour, M.; Mansour, A.T.; Abdelwahab, A.M.; Alprol, A.E. Metal Oxide Nanoparticles' Green Synthesis by Plants: Prospects in Phyto- and Bioremediation and Photocatalytic Degradation of Organic Pollutants. *Processes* **2023**, *11*, 3356, https://doi.org/10.3390/pr11123356.
23. Salova, A.; Mohealdeen, S.M.; Hussein, A.H.A.; Hasan, D.F.; Mushtaq, H.; Idan, A.H.; Fallah Amer, R. Phytochemical preparation of Zinc Stannate nanoparticles by using lemon and grapefruit peels for removal of cadmium ions. *Phys. Scr.* **2024**, *99*, 095925, https://doi.org/10.1088/1402-4896/ad6811.
24. Villagrán, Z.; Anaya-Esparza, L.M.; Velázquez-Carriles, C.A.; Silva-Jara, J.M.; Ruvalcaba-Gómez, J.M.; Aurora-Vigo, E.F.; Rodríguez-Lafitte, E.; Rodríguez-Barajas, N.; Balderas-León, I.; Martínez-Esquivias, F. Plant-Based Extracts as Reducing, Capping, and Stabilizing Agents for the Green Synthesis of Inorganic Nanoparticles. *Resources* **2024**, *13*, 70, https://doi.org/10.3390/resources13060070.
25. Ayyanaar, S.; Kesavan, M.P. One-pot biogenic synthesis of gold nanoparticles@saponins niosomes: Sustainable nanomedicine for antibacterial, anti-inflammatory and anticancer therapeutics. *Colloids Surf. A: Physicochem. Eng. Asp.* **2023**, *676*, 132229, https://doi.org/10.1016/j.colsurfa.2023.132229.
26. Jeevanandam, J.; Chan, Y.S.; Danquah, M.K. Biosynthesis of Metal and Metal Oxide Nanoparticles. *ChemBioEng Rev.* **2016**, *3*, 55–67, https://doi.org/10.1002/cben.201500018.
27. El-Seedi, H.R.; El-Shabasy, R.M.; Khalifa, S.A.M.; Saeed, A.; Shah, A.; Shah, R.; Iftikhar, F.J.; Abdel-Daim, M.M.; Omri, A.; Hajrahand, N.H.; Sabir, J.S.M.; Zou, X.; Halabi, M.F.; Sarhan, W.; Guo, W. Metal nanoparticles fabricated by green chemistry using natural extracts: biosynthesis, mechanisms, and applications. *RSC Adv.* **2019**, *9*, 24539-24559, https://doi.org/10.1039/c9ra02225b.
28. Aryanti, N.; Nafiunisa, A.; Kusworo, T.D.; Wardhani, D.H. Dye solubilization ability of plant derived surfactant from *Sapindus rarak* DC. extracted with the assistance of ultrasonic waves. *Environ. Technol. Innov.* **2021**, *22*, 101450, https://doi.org/10.1016/j.eti.2021.101450.
29. Prasad B, V.; Manjunatha, H.C.; Vidya, Y.S.; Manjunatha, S.; Munirathnam, R.; Shivanna, M.; Ningappa,C; Daruka Prasad, B; Sahana, R.; Manjunatha, K.; Wu, S.Y.; Sridhar, K.N. Oxygen evolution reaction kinetics and photoluminescence studies of zinc stannate ($ZnSnO_3$/Zn_2SnO_4) nanoparticles synthesized via *Aloebarbadensismiller* mediated route. *Mater. Sci. Eng. B* **2024**, *305*, 117427, https://doi.org/10.1016/j.mseb.2024.117427.
30. Hong, Y.; Wang, B.; Hu, S.; Lu, S.; Wu, Q.; Fu, M.; Gu, C.; Wang, Y. Preparation and photocatalytic performance of Zn_2SnO_4/ZIF-8 nanocomposite. *Ceram. Int.* **2023**, *49*, 11027-11037, https://doi.org/10.1016/j.ceramint.2022.11.298.
31. Bagheri, A.R.; Aramesh, N.; Hasnain, M.S.; Nayak, A.K.; Varma, R.S. Greener fabrication of metal nanoparticles using plant materials: A review. *Chem. Phys. Impact* **2023**, *7*, 100255, https://doi.org/10.1016/j.chphi.2023.100255.
32. Banjara, R.A.; Kumar, A.; Aneshwari, R.K.; Satnami, M.L.; Sinha, S.K. A comparative analysis of chemical vs green synthesis of nanoparticles and their various applications. *Environ. Nanotechnol. Monit. Manag.* **2024**, *22*, 100988, https://doi.org/10.1016/j.enmm.2024.100988.
33. Li, Z.; Zhou, Y.; Zhang, J.; Tu, W.; Liu, Q.; Yu, T.; Zou, Z. Hexagonal Nanoplate-Textured Micro-Octahedron Zn_2SnO_4: Combined Effects toward Enhanced Efficiencies of Dye-Sensitized Solar Cell and Photoreduction of CO_2 into Hydrocarbon Fuels. *Cryst. Growth Des.* **2012**, *12*, 1476-1481, https://doi.org/10.1021/cg201568q.
34. Sugihartono, I.; Isnaeni, I.; Mohar, R.S.; Widiasih, W. The Effects of Growth Time on Surface Morphology and Optical Band Gap Energy ZnO Thin Films. *J. Phys. Conf. Ser.* **2022**, *2377*, 012011, https://doi.org/10.1088/1742-6596/2377/1/012011.
35. Ibrahim, D.M.; Mahani, R.M.; Shaaban, M.N.; Maghraby, M.E.; Mahmoud, N.; Gaber, A.A. Synthesis of zinc stannate compounds utilizing natural cassiterite mineral. *Ceram. Int.* **2025**, *51*, 7728-7741, https://doi.org/10.1016/j.ceramint.2024.12.211.
36. Osman, A.I.; Zhang, Y.; Farghali, M.; Rashwan, A.K.; Eltaweil, A.S.; Abd El-Monaem, E.M.; Mohamed,

I.M.A.; Badr, M.M.; Ihara, I.; Rooney, D.W.; Yap, P.-S. Synthesis of green nanoparticles for energy, biomedical, environmental, agricultural, and food applications: A review. *Environ. Chem. Lett.* **2024**, *22*, 841-887, https://doi.org/10.1007/s10311-023-01682-3.

37. El Messaoudi, N.; Ciğeroğlu, Z.; Şenol, Z.M.; Kazan-Kaya, E.S.; Fernine, Y.; Gubernat, S.; Lopicic, Z. Green synthesis of $CuFe_2O_4$ nanoparticles from bioresource extracts and their applications in different areas: a review. *Biomass Conv. Bioref.* **2025**, *15*, 99-120, https://doi.org/10.1007/s13399-023-05264-9.
38. Afonso, I.S.; Cardoso, B.; Nobrega, G.; Minas, G.; Ribeiro, J.E.; Lima, R.A. Green synthesis of nanoparticles from olive oil waste for environmental and health applications: A review. *J. Environ. Chem. Eng*. **2024**, *12*, 114022, https://doi.org/10.1016/j.jece.2024.114022.

Publisher's Note & Disclaimer